CIVIL ENGINEERING JOURNAL

Article no. 6

THE CIVIL ENGINEERING JOURNAL 1-2024

RESEARCH ON THE DEVELOPMENT OF LOW-TEMPERATURE-RESISTANT FAST-CURING STRUCTURAL ADHESIVE AND STEEL PLATE STRENGTHENING CONCRETE BEAM FLEXURAL TEST

Guanhua Zhang[1], Chengzhe Song[1,2], Xihang Han[3] and Bo Lu[4]

1. *Liaoning Provincial Transportation Planning and Design Institute Co., Ltd, 110166, Shenyang, China; (E-mail: lnzgh123@163.com)*
2. *Liaoning Datong Highway Engineering Co., Ltd, 110111, Shenyang, China; (E-mail: songzhe0323@163.com)*
3. *Shenyang Jianzhu University, School of Transportation and Geomatics Engineering, Shenyang, 110168, China; (E-mail: hxihang@163.com)*
4. *Shenyang University of Chemical Technology, School of Material Science and Engineering, Shenyang, 110142, China; (E-mail: lubo608@sina.com)*

ABSTRACT

Steel plate strengthening method is a common, efficient, and mature reinforcement method that utilizes structural adhesive to bond steel plates with concrete components to work together. It takes advantage of the excellent tensile strength of steel plates to improve the mechanical properties of the original structure. However, epoxy-based structural adhesives are highly sensitive to the environment, and curing effect at low temperatures is a key issue. This study developed a low-temperature-resistant fast-curing structural adhesive (LTR-FCA) that can achieve rapid curing at low temperatures of -5 °C. The flexural performance of reinforced concrete beams strengthened with steel plates using LTR-FCA was compared with that using Normal Structural Adhesive (NSA). Experimental results indicated that LTR-FCA could rapidly cure at a low temperature of -5°C. Compared to NSA, which cures at room temperature, the use of LTR-FCA effectively delayed the debonding of the steel plates.

KEYWORDS

Epoxy resin structural adhesive, Low temperature rapid curing, Debonding failure, Steel plate strengthening method, Concrete structure

INTRODUCTION

The safety and durability of in-service concrete structures have always been hot topics in civil engineering. The main methods for repairing and strengthening concrete structures include enlarging the cross-section [1-4], bonding plates [5-8], or applying prestress [9-12].

The steel plate bonding method is widely studied and used due to its mature technology and effective reinforcement. R Thamrin et al. [13,14] investigated how different reinforcement methods and the lengths of steel plates affect the flexural strength of RC beams. The test results revealed that the length of steel plate application influenced the failure mode of the reinforced beams. Additionally, beams that failed due to debonding bore loads similar to the control beams. Yan et al.

[15] conducted a study to analyze the effects of steel plate thickness and U-shaped steel plate hoops on the failure mechanism and dynamic response of the structure. The result of the research indicates that as the bonded the steel plate thickness increased, the peak displacement and residual displacement in the mid-span decreased by 6.55% and 29.53%, respectively, and the residual flexural capacity increased by 25.02%. When U-shaped steel plate hoops were implemented, the residual flexural capacity of the reinforced beam was significantly improved, and both the peak displacement and residual displacement in the mid-span decreased. Thamrin et al. [16] studied the mechanical properties of reinforced concrete beams with steel plates bonded to the webs. The test variables included the ratio of longitudinal reinforcement and the position of the steel plates. The study emphasized the importance of avoiding steel plates debonding.

Structural adhesives play a crucial role in steel plate reinforcement technology, ensuring that the steel plates are tightly bonded to the structures to be reinforced, thereby enhancing the synergistic effect between them. Epoxy resin and curing agents are the main materials for bridge-strengthening adhesives [17-19]. Consequently, extensive research has been conducted on developing structural adhesives.

Wu et al. [20] evaluated the mechanical properties of two types of hydroxyl-terminated polyurethanes (HTPU1 and HTPU2) modified bisphenol A (DGEBA)/diethyl toluene diamine (DETDA) systems, specifically assessing the influence of phase structure on the overall performances of the resin at room temperature (RT) and cryogenic temperature (77 K). Mohammad et al. [21] studied the effects of carbon-based and silicon-based nanomaterials on the physical-chemical properties of a structural epoxy adhesive. The results showed that the addition of nanomaterials altered the chemical composition of the NE. In addition, impregnating the nanoparticles into NE affected its physical structure, resulting in an increase in porosity and a decrease in crystallinity with increasing wt.%. S Ranji et al. [22] conducted research on the synthesis of new urethane epoxy adhesives and their adhesive properties on different substrates. The findings revealed that compared to common DGEBA-based epoxy adhesives, the novel urethane-epoxy adhesive exhibited superior mechanical properties, specifically in terms of shear strength and elongation. Leena Karthikeyan et al. [23] developed a new type of room-temperature-cured epoxy resin and mixed it with different amounts of hydroxyl-terminated poly(etheretherketone)s (PEEKTOH), a thermoplastic toughening agent. The mixed resin was then cured using triethylenetetramine (TETA). Their research showed that the viscosity of the resin increased with the proportion of PEEKTOH in the epoxy matrix, which subsequently reduced the wetting characteristics. Moreover, the introduction of PEEKTOH phases into the mixture reduced the gel time from 175 minutes to 30 minutes.

However, epoxy resin adhesives are highly susceptible to environmental conditions, with the curing temperature being primarily determined by the reactivity of both the curing agent and the resin itself. In situations where the ambient temperature is below 0 °C, the adhesive may experience crystallization hardening and other related issues. Many current adhesives either cannot be fully cured at low temperatures or require extended curing times, which directly impact progress and quality of the project. Therefore, the development of low-temperature-resistant fast-curing structural adhesives (LTR-FCA) has always been a crucial topic within the field of engineering reinforcement.

Moussa et al. [24,25] discovered that the tensile properties of a commercial structural epoxy adhesive are greatly influenced by the curing temperature. At lower temperatures, the curing process slows down significantly, resulting in a corresponding reduction in the development rate of mechanical properties. At 0 °C, the curing process is either completely inhibited or fails to initiate altogether. Younes Jahani et al. [26] conducted a comprehensive experimental study to investigate the influence of temperature on the mechanical properties and glass transition temperature (T_g) of a structural epoxy adhesive. The results showed that the curing process (curing and post-curing) temperature had a positive impact when it was below the T_g, but had a negative impact when it exceeded the T_g. Ricardo Cruz et al. [27] studied the effects of the preparation, curing, and hygrothermal conditions on the viscoelastic response of a structural epoxy adhesive. The results showed that the preparation method had a significant impact on the tensile properties of the adhesive,

particularly on its viscoelastic response. Specimens that were degassed and cured at 20 °C exhibited lower creep deformations. However, specimens that were exposed to 98% relative humidity experienced tertiary creep before ultimately rupturing.

This study aims to prepare a low-temperature-resistant fast-curing structural adhesive (LTR-FCA) by adjusting the ratio of epoxy resin to low-temperature curing agents, and introducing toughening agents, promoters, and inorganic fillers as modifiers. Subsequently, flexural tests on reinforced concrete beams were conducted under different temperature conditions (-25°C, -5°C and 20°C), to investigate the bonding performance of LTR-FCA in low-temperature environments, and compare its adhesive effects with that of normal structural adhesives used under room temperature conditions.

DEVELOPMENT OF STRUCTURAL ADHESIVE FOR STEEL BONDING

Material composition

Epoxy resin curing agents commonly used include dicyandiamide, imidazole derivatives, anhydrides, and aromatic amines [28-31], among these curing agents typically require high or relatively high temperatures to effectively cure epoxy resin. At room temperature and low temperatures, mercaptan-based curing agents and thiourea-modified amine curing agents can achieve a rapid cure. There are numerous types of mercaptan-based curing agents [32-34], with common examples being liquid oligomers or multi-thiol compounds. The selection of accelerators varies depending on the structure of the mercaptan curing agent, resulting in differences in curing temperature and time.

Polythiol curing agent [35-37] is a type of multi-thiol that can be prepared by reacting β-mercaptopropionic acid with pentaerythritol to generate a multi-thiol ester. This ester is then heated and extended using a small amount of E-51 epoxy resin. The polythiol curing agent acts as a fast-curing agent at room temperature or low temperature, with low toxicity. When combined with an amine promoter, the epoxy resin can be cured within 1-5 minutes. Even under low temperatures (-20-0°C) and humid environments, the addition of promoter DMP-30 can also cure the epoxy resin. The curing time is 2-10 minutes, and the strength for use can be reached after 10-30 minutes. Full cure takes 7 days.

The main research and development ideas are: (a) By adjusting the ratio of epoxy resin E-51 and epoxy resin JD919, an epoxy resin that does not crystallize in a low temperature environment of -5 °C is formulated; (b) Fillers such as silica, white carbon black, and microbeads make the adhesive paste-like, with thixotropic and non-slippery properties during application, and reduce the linear expansion coefficient of the adhesive. (c) Toughgeners can improve the toughness and low-temperature resistance of the adhesive, and reduce the cure shrinkage. (d) Low-temperature curing agents (thiourea-modified aliphatic polyamines and polythiols) can promote the curing of the adhesive in a low-temperature environment of -5 °C or above, with good resistance to acids, bases, and water.

After multiple experiments, the optimal ratio of low-temperature-resistant fast-curing structural adhesive was obtained. Refer to Table 1 for details.

Tab. 1 - Recipe of structural adhesive for steel bonding (unit: g)

Type of glue	Materials	Component
A	Epoxy resin E-51	80.0
	Epoxy resin JD919	10.0
	polysulfide rubber	15.0
	coupling agent	2.0
	silica micro powder	98.0
	white carbon black	2.0
	microbeads	1.5
B	thiourea fatty polyamine	20.0
	polymeric mercaptan	10.0
	accelerator; promoter	3.0
	silica micro powder	31.0
	white carbon black	2.0
Proportion: A / B	100 / 32.5	

Material Properties

The material tests of low-temperature-resistant fast-curing structural adhesive (LTR-FCA) were carried out, and the average values of 5 specimens in each group were taken, as shown in Figure 1.

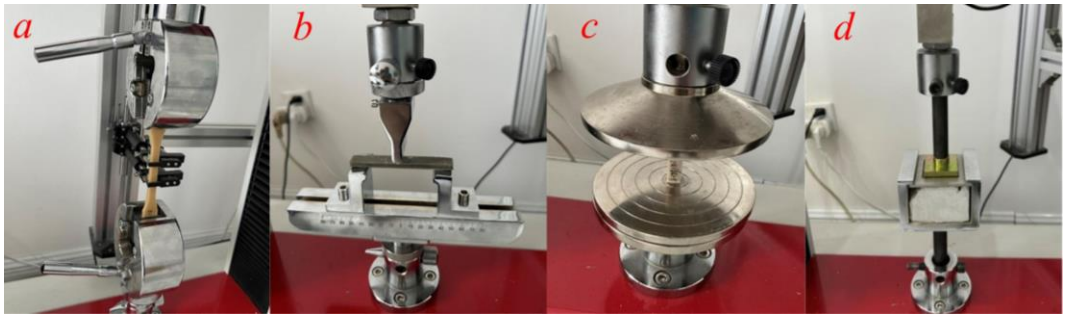

(a) Tensile test, (b) Flexural test, (c) Compressive test, (d) Test of normal tensile bond strength with concrete.

Fig.1 - Material Test

There are 2 types of test curing stages:

Curing stage I: At -5 °C, the curing period is 7 days, marked as 7d (-5 °C); According to the specifications [38], during this curing stage, the strength of the glue should reach 90% of the technical indicators.

Curing stage II: After curing for 7 days at -5 °C, it shall be cured for another 3 days at 23±2 °C, marked as 7d (-5 °C) + 3d (23±2 °C). At the same time, the specifications stipulate that after the curing stage, the strength of the rubber should meet the requirements of technical indicators.

Table 2 shows the test results of the material properties of LTR-FCA under the two conditions mentioned above.

Tab. 2 - Material properties of LTR-FCA

Material index	7d(-5 °C)		7d(-5 °C) + 3d(23±2 °C)	
	Indicator	Test value	Indicator	Test value
Tensile strength (MPa)	≥ 27.0	39.3	≥ 30	43.2
Tension elastic modulus (MPa)	≥ 2.9(×10^3)	5.2	≥ 3.2(×10^3)	5.5
Elongation (%)	≥ 1.1	1.4	≥ 1.2	1.4
Flexural strength (MPa)	≥ 40.5	65.2	≥ 45.0	95.7
Compressive strength (MPa)	≥ 58.5	63.7	≥ 65.0	74.8
Tensile shear strength of steel-steel (MPa)	≥ 13.5	13.5	≥ 15.0	15.3
Steel-steel T impact stripping length (mm)	≤ 27.8	0.0	≤ 25.0	0.0
Tensile strength of steel-steel butt bond (MPa)	≥ 29.7	30.3	≥ 33.0	34.1
The tensile bond strength with concrete (MPa)	≥ 2.2	2.6	≥ 2.5	3.0
Non-volatile matter content (%)	≥ 89.1	99.6	≥ 99.0	99.6

From Table 2, it can be seen that all material performance tests meet the requirements of the technical specifications, especially with regards to tensile strength and flexural strength, which reached 43.2MPa and 95.7MPa respectively, demonstrating excellent material performance.

TEST OF STRENGTHENING CONCRETE BEAMS WITH STRUCTURAL ADHESIVES

This study has developed a low-temperature-resistant fast-curing structural adhesive (LTR-FCA) for steel bonding in concrete reinforcement, aiming to improve the construction convenience and reliability of the structural adhesive in low-temperature environments. In addition, to verify the superiority of its materials and mechanical properties, the strengthening beam was conducted flexural test to compare and analyze it with normal structural adhesives (NSA).

A total of 3 groups of test beams were designed, with dimensions of 2900mm in length, 280mm in width, and 340mm in height. The three groups of specimens were tested at 20 °C, -5 °C, and -25 °C. Each group consists of 3 test beams, one of which is a normal reinforced concrete beam without steel plate bonding, while the other two beams are strengthened with NSA and LTR-FCA, respectively. Strengthening beams with 1600 mm×200 mm×3 mm Q235 steel plates at the bottom, and the thickness of the adhesive layer is controlled at 2mm. The main parameters of the test beams are shown in Table 3.

Tab. 3 - Main parameters of the test beams

Group	Label	Type of structural adhesives	Steel plate thickness (mm)	Cultivation method	Testing temperature (°C)
I	CB+20	/	/	/	20
	NTB+20	NSA	3	7d (23±2 °C)	
	LTB+20	LTR-FCA	3	7d (-5 °C) + 3d (23±2 °C)	
II	CB-5	/	/	/	-5
	NTB-5	NSA	3	7d (23±2 °C)	
	LTB-5	LTR-FCA	3	7d (-5 °C) + 3d (23±2 °C)	
III	CB-25	/	/	/	-25
	NTB-25	NSA	3	7d (23±2 °C)	
	LTB-25	LTR-FCA	3	7d (-5 °C) + 3d (23±2 °C)	

The test beams were crafted from C40 commercial concrete, and the concrete cube strength (f_{cu}) was determined through experiments conducted at 20 °C, -5 °C, and -25 °C, resulting in values of 48.7MPa, 44.0MPa, and 52.3MPa, respectively. The longitudinal tensile steel bars incorporate four HRB400 steel bars with a diameter of 28mm (f_y = 420MPa). The stirrups and bracket steel bars

feature HRB400 steel bars with a diameter of 10mm (f_y = 448MPa). The steel plate is fashioned from Q235 steel with a yield strength of 235 MPa. Both the steel bars and steel plates are assumed to have an elastic modulus of 200 GPa. The configuration of reinforcement in the test beams is presented in Figure 2.

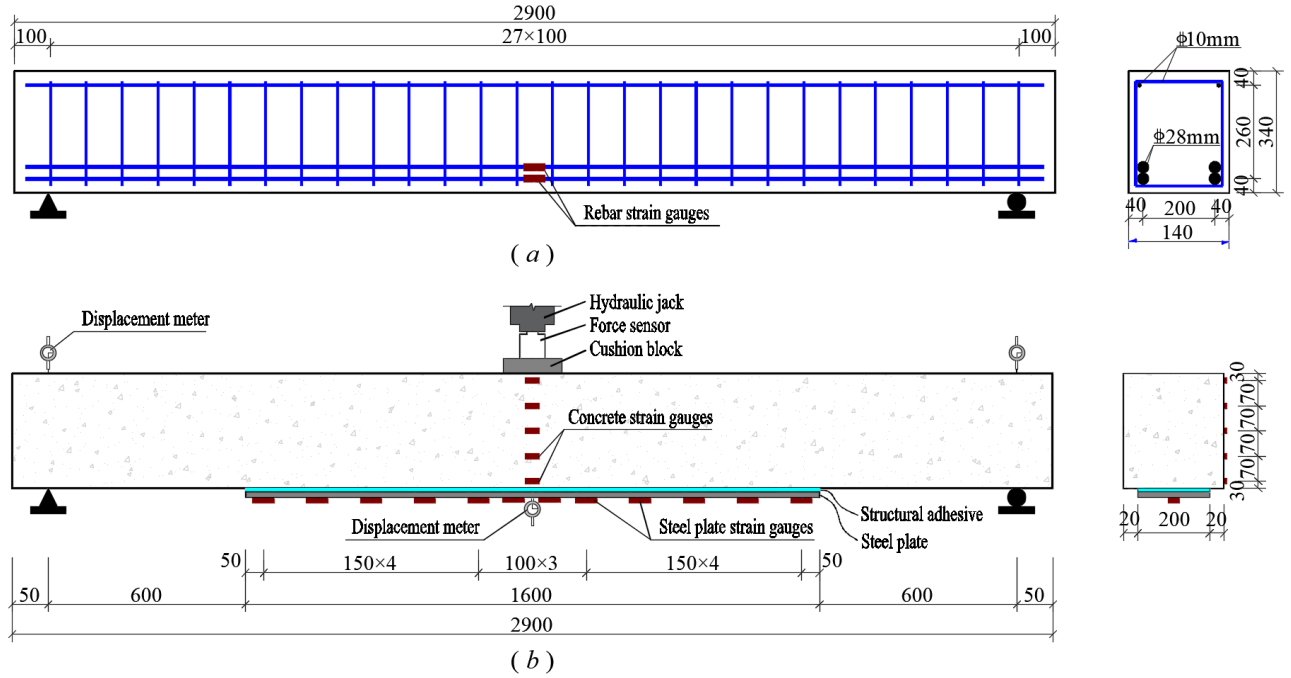

Fig. 2 - Design of test beam (unit: mm)

Displacement meters were arranged at the support and mid-span positions of the test beam, and concrete strain gauges were installed along the height of the beam at the mid-span position. Rebar Strain gauges were adhered to the longitudinal reinforcement at the mid-span position. Steel plate strain gauges were affixed to the steel plate at the bottom of the beam to monitor the strain values in real-time during the loading process and determine whether the steel plate has peeled off.

After the test beams were poured and cured for 90 days, the steel plate was pasted. The specific pasting method and curing process are as follows:

(1) NTB+20, NTB-5, NTB-25: Paste and cure for 7 days at (23±2) °C.

(2) LTB+20, LTB-5, LTB-25: Paste and cure for 7 days at -5 °C, then cure for 3 days at (23±2) °C.

After the completion of the curing process, the test beams were placed in an environmental simulation chamber, and after 4 hours at the predetermined temperature, a uniaxial three-point load was applied. The load was applied in a displacement gradient manner through a jack.

FAILURE PHENOMENON AND RESULT ANALYSIS OF TEST BEAMS

Load – displacement curve and failure process

A total of 9 beams were tested, respectively at 20 °C, -5 °C and -25 °C. The main variables in the experiment were the type of adhesive and the test temperature.

The main experimental results are shown in Table 4. By bonding steel plates to the bottom surface of the concrete beam with structural adhesive, the steel plates and the test beam were integrated, effectively bearing the stress at the bottom of the beam, enhancing the stiffness of the beam, and increasing the cracking load of the beam. The cracking load of the reinforced test beams increased by 10~20 kN, and the propagation of bottom cracks in the concrete beams was effectively delayed before the steel plates peeled off.

Tab - 4 Main experimental results

Label	Cracking load (kN)	Peeling load of steel plate (kN)	Ultimate load of beam (kN)
CB+20	49.7	/	429.7
NTB+20	61.2	261.9	418.1
LTB+20	69.6	309.7	422.1
CB-5	48.3	/	424.8
NTB-5	62.0	287.1	412.4
LTB-5	70.5	311.4	419.3
CB-25	47.5	/	424.3
NTB-25	59.5	290.2	442.9
LTB-25	69.4	321.7	425.0

The strengthened beams in the test all experienced steel plate peeling before the beam failure, with NTB-5, LTB+20 and LTB-25 as examples, which is illustrated in Figure 3. Ultimately, both the control beams and the reinforced beams experienced flexural failure, with CB-25, NTB-25 and LTB-25 as examples, which is illustrated in Figure 4.

(a) NTB-5

(b) LTB+20

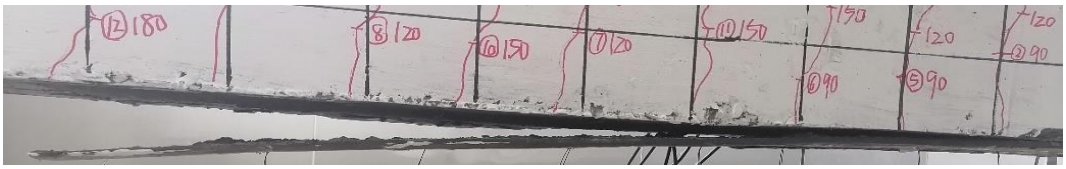

(c) LTB-25

Fig. 3 - Peeling of steel plate

(a) CB-25

(b) NTB-25

Fig. 4 - The crack distribution of test beams

(c) LTB-25

Fig. 4 - The crack distribution of test beams

Figure 5 shows the load-displacement relationship of the test beams at different temperatures. When the test temperature was reduced from 20°C to -5°C and -25°C, the peel loads of both types of structural adhesives increased. For the test beams NTB-5 and NTB-25 using NSA, their peel loads increased by 9.6% and 10.8% respectively compared to NTB+20; while for the test beams LTB-5 and LTB-25 using LTR-FCA, the increase was 0.5% and 3.9% respectively compared to LTB+20. Compared to NSA, LTR-FCA has a lower sensitivity to temperature changes, demonstrating better curing stability.

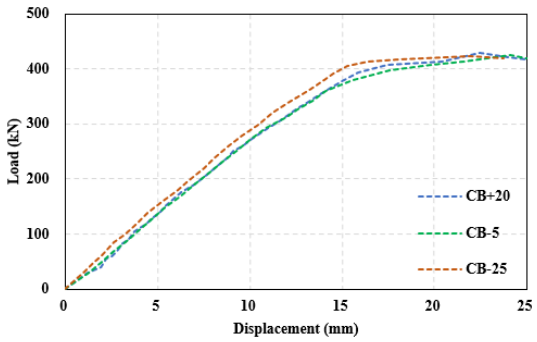

(a) CB

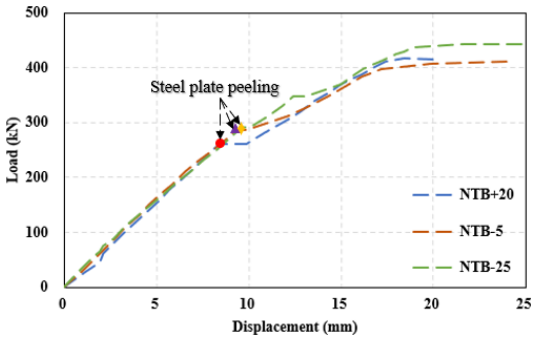

(b) NSA

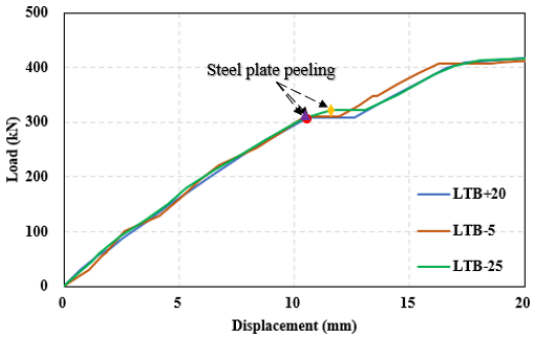

(c) LTR-FCA

Fig. 5 - Load – displacement curve

As shown in Figure 6, at different test temperatures, the peeling load of the test beams reinforced with LTR-FCA was generally higher than that of the beams reinforced with NSA. Specifically, at -25°C, the peeling load of LTR-FCA increased by 10.78% compared to NSA; it increased by 8.50% at -5°C; and at +20°C, it increased by 18.21%. This indicates that the LTR-FCA can effectively cure even in low-temperature environments and demonstrates superior bonding performance.

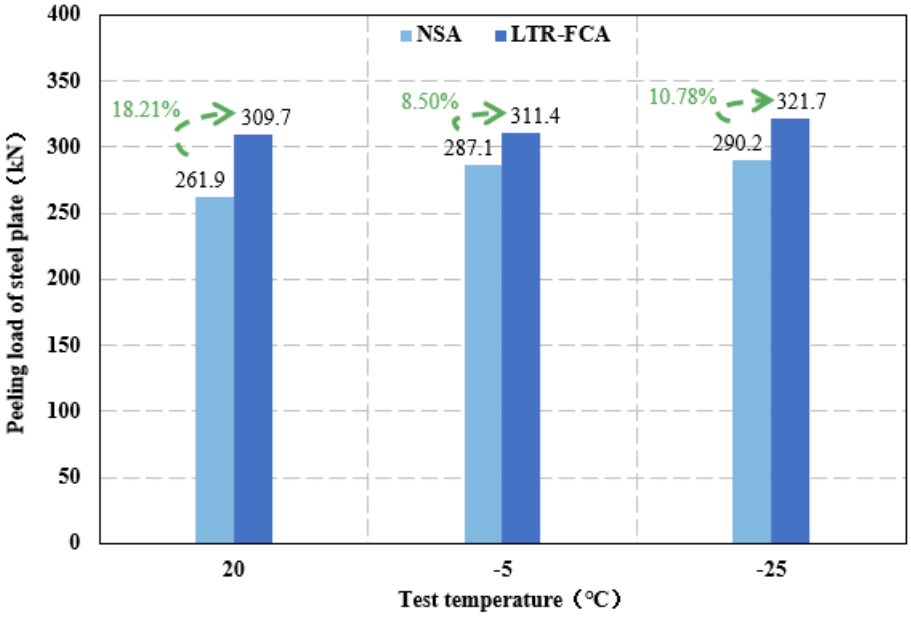

Fig. 6 - Peeling load of steel plate (kN)

In the later stages of the test beams after the steel plate was peeled off, the flexural capacity of the strengthened beams was not significantly different from the control beams. This is because the flexural load-bearing capacity of the beam is mainly determined by the dimensions of the beam, the number of longitudinal reinforcements, and the strength of the concrete. In addition, the test beams exhibited typical flexural failure.

Strain

The curves of strain versus load for test beams are shown in Figure 7. It can be seen from Figure 7 that during the initial loading period, the neutral axis remained stable near the mid-span of the beam, and the cross-section approximately met the plane section assumption. As the load increased, the cross-section cracked, and the neutral axis gradually shifted towards the compressive zone. Overall, however, the strain condition remained largely consistent with the plane section assumption.

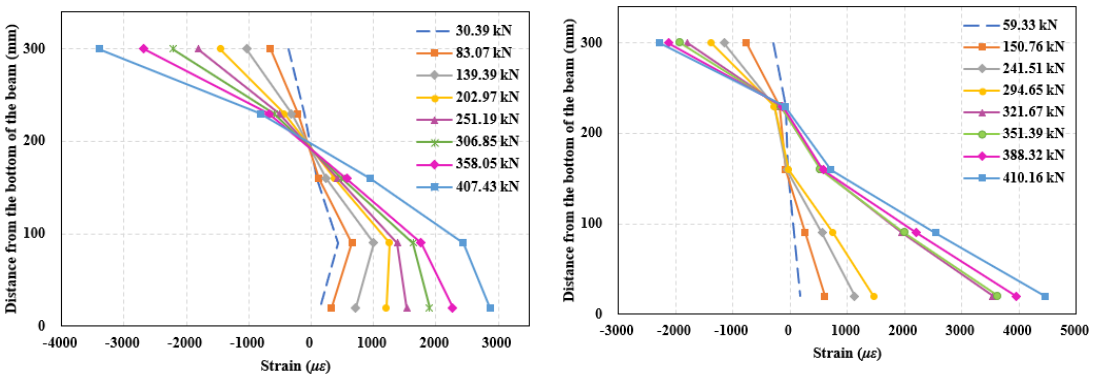

(a) CB+20 *(b) LTB-25*

Fig. 7 - Load-strain curve in the mid-span section of the test beam

Figure 8 shows the strain response curves of longitudinal reinforcement under different loads. It is observed that the trend of strain variation in the longitudinal reinforcement of the test beams with increasing load is consistent with their load-displacement curves. When the steel plate peeling occurs, the strain in the longitudinal reinforcement of the strengthened beams increases sharply,

ranging from 476 με (NTB-5) to 746 με (NTB+20). This indicates that once the steel plate peeling, it loses its load-bearing capacity, leading to a greater load on the longitudinal reinforcement and thus a significant increase in strain. All test beams ultimately experienced the yielding of longitudinal reinforcement and the crushing of concrete in the compression zone, demonstrating good ductility and exhibiting a typical flexural failure mode.

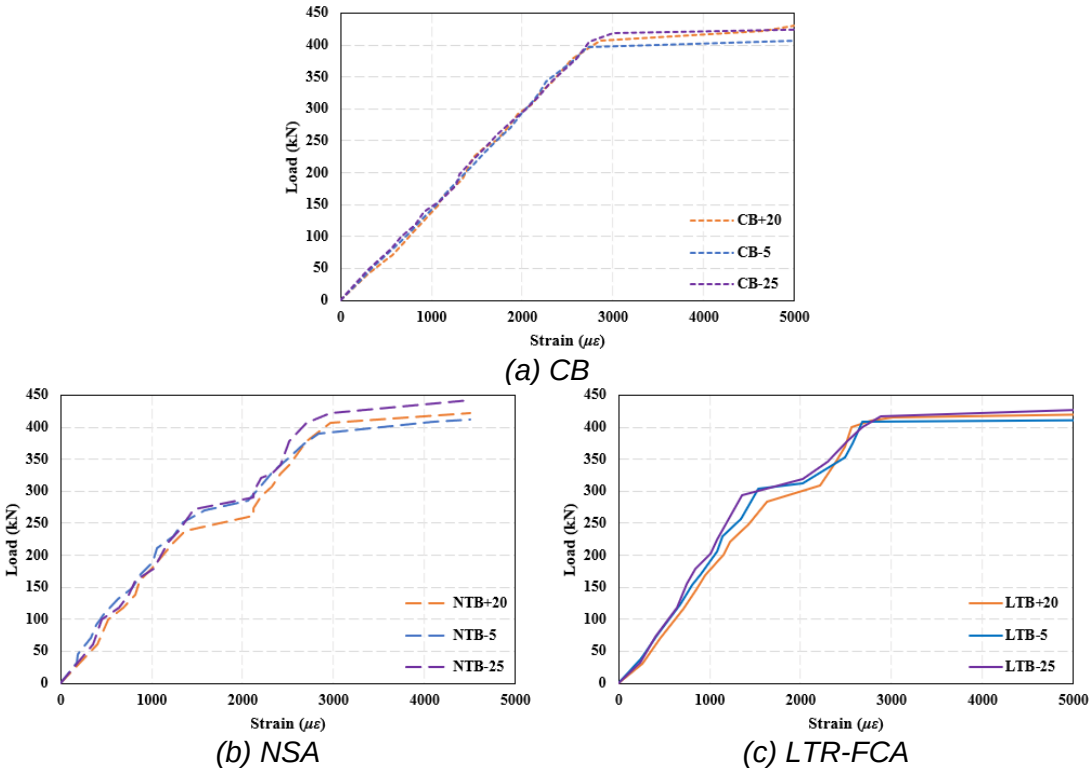

(a) CB

(b) NSA

(c) LTR-FCA

Fig. 8 - Load-strain response curves of the longitudinal reinforcements

Figure 9 shows the relationship curve between the steel plate strain and load for some of the test beams. It can be observed that as the load gradually increases, the strain in the steel plate correspondingly rises. This is particularly noticeable at the mid-span position of the steel plate, where the strain increment is significantly higher than at the ends, while the stress at the ends remains almost unchanged; when the end steel plates become detached, the stress at the mid-span position drops rapidly. This indicates that during the loading process, the steel plate mainly bears shear forces at the mid-span, while it primarily withstands normal stress at the ends. It is recommended that in practical engineering applications, bolting at the ends of steel plates should be used for anchoring to delay the peeling phenomenon.

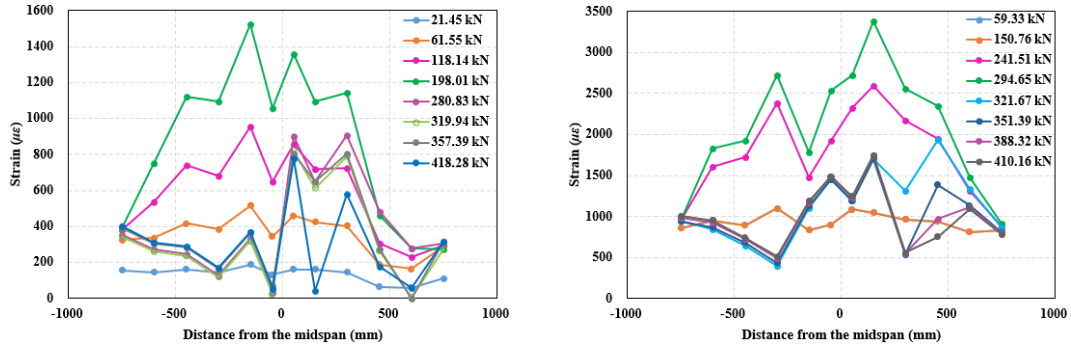

(a) NTB+20

(b) LTB-25

Fig. 9 - Load-strain curve in steel plates of the test beam

As shown in Figure 10, when the test temperature was reduced from 20°C to -25°C, the loads corresponding to the maximum steel plate strain for beams using NSA were 261.9kN, 287.1kN, and 290.2kN, respectively, while for beams using LTR-FCA, the loads were 309.7kN, 311.4kN, and 321.7kN, respectively. These results indicate that as the test temperature decreases, the maximum strain of the steel plate increases, consistent with the relationship between peel load and temperature. This phenomenon can be explained by the principle of thermal expansion and contraction: the reduction in temperature causes the inter-particle spacing between the substrate and the adhesive to decrease, enhancing their bonding strength. And at the same test temperature, the maximum strain of steel plate LTR-FCA (1753 με~2723 με) is greater than that of NSA (1347 με~1893 με), which is consistent with the relationship between the peeling load of the two adhesives, exhibits better bond strength of LTR-FCA.

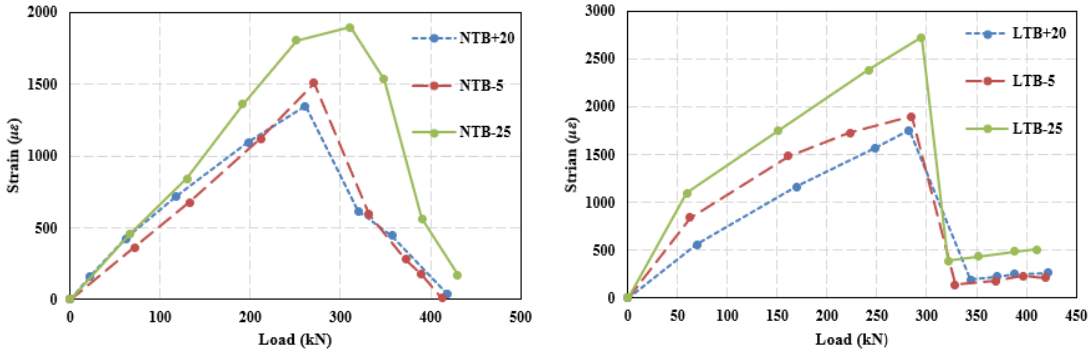

(a) Load strain at midspan of the NSA steel plate

(b) Load strain at midspan of the LTR-FCA steel plate

Fig. 10 - Load-strain curve in steel plates of the test beam

CONCLUSION

This study developed a low-temperature-resistant fast-curing structural adhesive for winter construction and tested its mechanical properties. Additionally, experimental research on the application of structural adhesives to reinforce concrete was conducted. The main conclusions are as follows:

(1) By bonding steel plates to the bottom surface of concrete beams with structural adhesive, the steel plates and the test beams are integrated to effectively bear the stress at the bottom of the beam. This method enhances the stiffness of the beam and increases its cracking load. It also effectively delays the expansion of cracks at the bottom of the concrete beam before the steel plates peel off.

(2) For the NTB-5 and NTB-25 beams using NSA, the peeling load increased by 9.6% and 10.8% compared to NTB+20. While for LTB-5 and LTB-25 beams using LTR-FCA, the peeling load increased by 0.5% and 3.9% compared to LTB+20. Whether it is NSA or LTR-FCA, their peel load shows a certain trend of increasing with the decrease of the test temperature.

(3) At 20 °C, -5 °C, and -25 °C, the peeling load of LTR-FCA is 18.21%, 8.50%, and 10.57% higher than that of NSA, respectively. That is, at the same test temperature, the peeling load of LTR-FCA is always higher than that of NSA. This reflects the good effect of LTR-FCA on the reinforcement of concrete structures.

(4) The developed LTR-FCA can effectively cure in low-temperature environments and possesses excellent material properties and adhesive strength. Considering that the ends of steel plates primarily bear normal stress, it is recommended to use bolt anchoring at the ends of steel plates in engineering applications to mitigate the peeling phenomenon.

ACKNOWLEDGEMENTS

This research was funded by the Transportation Science and Technology Project of Liaoning Provincial (202129).

REFERENCES

[1] X. Gao, K. Wu, Y. Guo, Y. Zhao, J. Guo, Experimental and numerical study on flexural behaviors of damaged RC beams strengthened with UHPC layer using the bonding technology of post-installed reinforcing bar, Construction and Building Materials. 391 (2023) 131835, doi: 10.1016/j.conbuildmat.2023.131835.

[2] M.M.A. Kadhim, A. Jawdhari, W. Nadir, A. Majdi, Experimental study on RC beams strengthened in flexure with CFRP-Reinforced UHPC overlays, Engineering Structures. 285 (2023) 116066, doi: 10.1016/j.engstruct.2023.116066.

[3] W. Nadir, M.M.A. Kadhim, A. Jawdhari, A. Fam, A. Majdi, RC beams strengthened in shear with FRP-Reinforced UHPC overlay: An experimental and numerical study, Structures. 53 (2023) 693-715, doi: 10.1016/j.istruc.2023.04.117.

[4] D. Mirdan, A.R. Saleh, Flexural performance of reinforced concrete (RC) beam strengthened by UHPC layer, Case Studies in Construction Materials. 17 (2022) e1655, doi: 10.1016/j.cscm.2022.e01655.

[5] X. He, C. Zhou, M. Lv, Y. Wang, Y. Liu, Interfacial stresses of beams hybrid strengthened by steel plate with outside taper and FRP pocket, Journal of Building Engineering. 75 (2023) 107034, doi: 10.1016/j.jobe.2023.107034.

[6] S. Hadi, E. Kazeminezhad, S. Safakhah, Full-scale experimental evaluation of flexural strength and ductility of reinforced concrete beams strengthened with various FRP mechanisms, Structures. 43 (2022) 1160-1176, doi: 10.1016/j.istruc.2022.07.011.

[7] M.J. Jedrzejko, J. Tian, S.S. Zhang, Y. Ke, X.F. Nie, Y.M. Yang, Strengthening of RC beams in shear with novel near-surface mounted (NSM) U-shaped fiber-reinforced polymer (FRP) composites, Engineering Structures. 292 (2023) 116479, doi: 10.1016/j.engstruct.2023.116479.

[8] D. Guo, H. Zhou, H. Wang, J. Dai, Effect of temperature variation on the plate-end debonding of FRP-strengthened steel beams: Coupled mixed-mode cohesive zone modeling, Engineering Fracture Mechanics. 270 (2022) 108583, doi: 10.1016/j.engfracmech.2022.108583.

[9] Z. Wang, J. Xie, J. Li, P. Liu, C. Shi, Z. Lu, Flexural behaviour of seawater–sea sand concrete beams reinforced with GFRP bars: Effects of the reinforcement ratio, stirrup ratio, shear span ratio and prestress level, Journal of Building Engineering. 54 (2022) 104566, doi: 10.1016/j.jobe.2022.104566.

[10] H. Wang, Z. Bian, M. Chen, L. Hu, Q. Wu, Flexural strengthening of damaged steel beams with prestressed CFRP plates using a novel prestressing system, Engineering Structures. 284 (2023) 115953, doi: 10.1016/j.engstruct.2023.115953.

[11] W. Du, C. Yang, Y. Pan, Y. Chen, H. Zhang, Study on the flexural behaviours of precracked hollow core beams strengthened with core filling and unbonded prestressing steel strands, Engineering Structures. 274 (2023) 115075, doi: 10.1016/j.engstruct.2022.115075.

[12] J. Deng, K. Rashid, X. Li, Y. Xie, S. Chen, Comparative study on prestress loss and flexural performance of rectangular and T beam strengthened by prestressing CFRP plate, Composite Structures. 262 (2021) 113340, doi: 10.1016/j.compstruct.2020.113340.

[13] R. Thamrin, Effect of strengthening method and development length on flexural strength of rc beams with steel plates, Journal of Engineering Science and Technology. 13 (11) (2018) 3781-3794.

[14] R. Thamrin, R.P. Sari, Flexural Capacity of Strengthened Reinforced Concrete Beams with Web Bonded Steel Plates, Procedia Engineering. 171 (2017) 1129-1136, doi: 10.1016/j.proeng.2017.01.474.

[15] X. Yan, T. Zheng, C. Lin, G. Lan, H. Mao, Experimental Research on the Impact Resistance of Partially Precast Concrete Beams Strengthened with Bonded Steel Plates, in: Applied Sciences, 2023, p.

[16] R. Thamrin, Zaidir, A. Wahyuni, Shear capacity of reinforced concrete beams strengthened with web bonded steel bars or steel plates, Results in Engineering. 17 (2023) 100953, doi: 10.1016/j.rineng.2023.100953.

[17] C. Liu, Y. He, M. Sun, X. Zhang, B. Zhang, X. Bai, Influence of epoxy resin species on the curing behavior and adhesive properties of cyanate Ester/Poly(aryl ether nitrile) blends, Polymer. 288 (2023) 126450, doi: 10.1016/j.polymer.2023.126450.
[18] F. Zhu, Q. Fu, M. Yu, J. Zhou, N. Li, F. Wang, Synthesis and curing properties of multifunctional castor oil-based epoxy resin, Polymer Testing. 122 (2023) 108017, doi: 10.1016/j.polymertesting.2023.108017.
[19] J. Wei, Y. Duan, H. Wang, W. Zhang, Study on copolymerization modification and properties of bio-based trifunctional diphenolic acid epoxy resin by CE and DPR, Polymer. 284 (2023) 126308, doi: 10.1016/j.polymer.2023.126308.
[20] T.Y.N.G. Wu, Cryogenic mechanical properties of epoxy resin toughened by hydroxyl-terminated polyurethane, Polymer Testing. 74 (2019).
[21] M. Al-Zu'Bi, L. Anguilano, M. Fan, Effect of incorporating carbon- and silicon-based nanomaterials on the physico-chemical properties of a structural epoxy adhesive, Polymer Testing. 128 (2023) 108221, doi: 10.1016/j.polymertesting.2023.108221.
[22] S. Ranji, M.C. Lee, Study on synthesizing new urethane epoxy adhesives and their adhesive properties on different substrates, International Journal of Adhesion & Adhesives (2022) 117A.
[23] L. Karthikeyan, T.M. Robert, D. Mathew, D.D. Suma, D. Thomas, Novel epoxy resin adhesives toughened by functionalized poly (ether ether ketone) s, International Journal of Adhesion and Adhesives. 106 (2021).
[24] O. Moussa, A.P. Vassilopoulos, J. de Castro, T. Keller, Early-age tensile properties of structural epoxy adhesives subjected to low-temperature curing, International Journal of Adhesion and Adhesives. 35 (2012) 9-16, doi: 10.1016/j.ijadhadh.2012.01.023.
[25] O. Moussa, A.P. Vassilopoulos, T. Keller, Effects of low-temperature curing on physical behavior of cold-curing epoxy adhesives in bridge construction, International Journal of Adhesion and Adhesives. 32 (2012) 15-22, doi: 10.1016/j.ijadhadh.2011.09.001.
[26] R. Cruz, L. Correia, S. Cabral-Fonseca, J. Sena-Cruz, Effects of the preparation, curing and hygrothermal conditions on the viscoelastic response of a structural epoxy adhesive, International Journal of Adhesion and Adhesives. 110 (2021) 102961, doi: 10.1016/j.ijadhadh.2021.102961.
[27] Y. Jahani, M. Baena, C. Barris, R. Perera, L. Torres, Influence of curing, post-curing and testing temperatures on mechanical properties of a structural adhesive, Construction and Building Materials. 324 (2022) 126698, doi: 10.1016/j.conbuildmat.2022.126698.
[28] J. Kamalipour, M.H. Beheshty, M.J. Zohuriaan-Mehr, Novel phosphonated hardeners derived from diamino diphenyl sulfone for epoxy resins: Synthesis and one-pack flame-retardant formulation alongside dicyandiamide, Polymer Degradation and Stability. 199 (2022) 109917, doi: 10.1016/j.polymdegradstab.2022.109917.
[29] S. Lin, G. Lai, M. Chen, L. Su, J. Lan, W. Zhong, H. Zhang, Boosting both flame retardancy and mechanical properties of carbon fiber/epoxy composites via polycyclic phosphorus-nitrogen imidazole derivative, Chemical Physics Letters. 805 (2022) 139946, doi: 10.1016/j.cplett.2022.139946.
[30] X. Liu, J. Zhou, M. Wu, S. Liu, J. Zhao, Design and synthesis of anhydride-terminated imide oligomer containing phosphorus and fluorine for high-performance flame-retarded epoxy resins, Chemical Engineering Journal. 461 (2023) 142063, doi: 10.1016/j.cej.2023.142063.
[31] J. Li, Z. Weng, Q. Cao, Y. Qi, B. Lu, S. Zhang, J. Wang, X. Jian, Synthesis of an aromatic amine derived from biomass and its use as a feedstock for versatile epoxy thermoset, Chemical Engineering Journal. 433 (2022) 134512, doi: 10.1016/j.cej.2022.134512.
[32] H. Zhang, J. Gao, Z. Guo, X. Wang, Q. Li, Z. Miao, The influence of the helical twisting power on the bistable electro-optical performance of the liquid crystalline epoxide/mercaptan /negative-dielectric-anisotropy cholesteric liquid crystal composite films, Optical Materials. 142 (2023) 114091, doi: 10.1016/j.optmat.2023.114091.
[33] F. Ahangaran, M. Hayaty, A.H. Navarchian, Y. Pei, F. Picchioni, Development of self-healing epoxy composites via incorporation of microencapsulated epoxy and mercaptan in poly(methyl methacrylate) shell, Polymer Testing. 73 (2019) 395-403, doi: 10.1016/j.polymertesting.2018.11.041.

[34] W. Shen, L. Wang, T. Zhong, G. Chen, C. Li, M. Chen, C. Zhang, L. Zhang, K. Li, Z. Yang, H. Yang, Electrically switchable light transmittance of epoxy-mercaptan polymer/nematic liquid crystal composites with controllable microstructures, Polymer. 160 (2019) 53-64, doi: 10.1016/j.polymer.2018.11.022.
[35] Z. Zhang, F. Gao, L. Li, L. Wei, Z. Su, H. Li, Y. Liu, H. Liu, Y. Liu, Performance study of an epoxy–polythiol curing system for local insulating spraying based on the imbalance stoichiometric ratio, Materials Letters. 351 (2023) 135123, doi: 10.1016/j.matlet.2023.135123.
[36] Z. Belbakra, Z.M. Cherkaoui, X. Allonas, Photocurable polythiol based (meth)acrylate resins stabilization: New powerful stabilizers and stabilization systems, Polymer Degradation and Stability. 110 (2014) 298-307, doi: 10.1016/j.polymdegradstab.2014.09.012.
[37] Y.C. Yuan, M.Z. Rong, M.Q. Zhang, Preparation and characterization of microencapsulated polythiol, Polymer. 49 (10) (2008) 2531-2541, doi: 10.1016/j.polymer.2008.03.044.
[38] MOHURD, Technical code for safety appraisal of engineering structural strengthening materials, in: GB 50728 - 2011, China Architecture & Building Press.